Quantum Control of Wave Packet Evolution with Tailored Femtosecond Pulses

Bern Kohler, Vladislav V. Yakovlev, Jianwei Che, Jeffrey L. Krause, Michael Messina, and Kent R. Wilson
Department of Chemistry and Biochemistry, University of California, San Diego, La Jolla, California 92093-0339

Nikolaus Schwentner
Department of Physics, Freie Universität Berlin, Arnimallee 14, D-14195 Berlin, Germany

Robert M. Whitnell
Department of Chemistry, Guilford College, Greensboro, North Carolina 27410

YiJing Yan
Department of Chemistry, Hong Kong University of Science and Technology, Kowloon, Hong Kong
(Received 2 December 1994)

Using theory to guide the choice of pulse shape, we have synthesized frequency-chirped laser pulses and used them to control the evolution of vibrational wave packets on the B excited state of iodine. A negatively chirped pulse produces a wave packet at the target time localized about an internuclear position and momentum of our choice. An approximately time-reversed pulse, however, produces a delocalized wave packet. The experimental results are in very good qualitative agreement with quantum simulations.

PACS numbers: 33.80.–b, 32.80.Qk, 42.50.Vk

The goal of quantum control is to use light to drive matter to a desired target, or outcome [1–8]. Several theoretical approaches to quantum control have been suggested, and recent experiments have demonstrated that the technology now exists to realize quantum control in the laboratory [9–13]. The unifying theme in all of the current theoretical and experimental schemes is the optimal use of the coherence of laser light to manipulate the quantum mechanical phase relationships among the eigenstates of matter. In this Letter we report on our joint theoretical-experimental results in controlling the vibrational wave packet dynamics of a diatomic molecule using tailored femtosecond pulses.

Our objective is to control the evolution of a vibrational wave packet on an electronic excited state of the iodine molecule [7,13], as illustrated schematically in Fig. 1. The molecule begins in a thermal distribution of vibrational levels in its ground electronic state, labeled X. The target distribution is chosen to be a minimum uncertainty Gaussian wave function on the B electronic excited state such that $\Delta x \Delta p = \hbar/2$, where Δx is the standard deviation in position and Δp is the standard deviation in momentum. The spread of the target in position and momentum is given by the formulas $\Delta x = \sqrt{\hbar/2m\omega}$ and $\Delta p = \sqrt{m\omega\hbar/2}$, where m is the reduced mass of the iodine molecule and the parameter ω (units of frequency) was chosen to correspond to 250 cm^{-1}. The target is centered about a chosen position (0.372 nm) and a chosen momentum (corresponding to a kinetic energy of 50 meV). In this case, the momentum is negative, meaning that the iodine atoms are moving toward each other. The target is achieved by using a tailored, ultrashort light field to create an initial wave packet that evolves under the influence of the molecular Hamiltonian to yield a wave packet that has maximum overlap with the target distribution at a later time. To reach the target in a reasonable amount of time, the electric field is allowed to be nonzero only during a temporal interval of our choice (550 fs, in the present case). Thus, the task of theory is to find the electric field $E(t)$ that best steers the system to our chosen target at the chosen time. We note that to achieve this target, the optimal field must overcome the wave packet spreading which ordinarily occurs in anharmonic potentials.

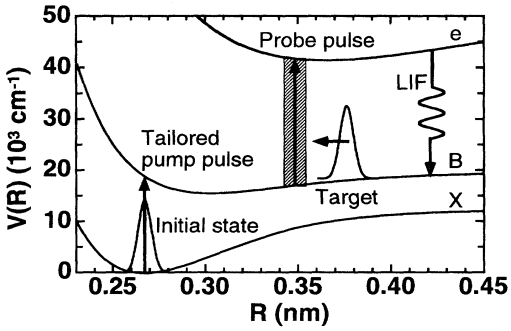

FIG. 1. Schematic of the iodine reflectron: A tailored femtosecond pulse creates a vibrational wave packet on the B excited state of iodine which evolves to produce a localized target state at a later time. The wave packet evolution is monitored by exciting the wave packet to the higher-lying e state with a second ultrashort pulse which opens up a "window" in internuclear distance (shown schematically by the striped box). The experimental signal is the total laser-induced fluorescence (LIF) from the e state as a function of delay between the pump and probe pulses, allowing detection of the wave packet density in a region of internuclear distance selected by the probe wavelength.

 0031-9007/95/74(17)/3360(4)$06.00

We have termed the scenario in Fig. 1 the "molecular reflectron," because the vibrational wave packet must reflect from the outer wall of the potential to reach the target region with a negative momentum [7]. We have previously described the theoretical formalism used to predict the globally optimal field for this example in the weak response (i.e., perturbative) limit [5–8]. Its dominant characteristic is a negative chirp, which excites the higher energy portions of the wave packet before the low energy ones. Classically, the higher energy components of the wave packet have longer vibrational periods than those with lower energy, due to the B state anharmonicity. Thus, by launching the higher energy components first, the lower energy components with shorter vibrational periods "catch up" to the higher energy components in the target region and interfere with them at the target time to produce the narrow target wave packet. We emphasize that although the optimal field for the reflectron is simple, and the mechanism by which it acts can be readily understood, the theory does not enforce *a priori* a particular pulse shape. In fact, the shape of the field is totally unconstrained within the selected time interval, and the theory discovers the simple chirped form automatically.

The apparatus we constructed to perform the reflectron experiment is illustrated schematically in Fig. 2. To obtain pump pulses tunable throughout the $B \leftarrow X$ absorption band of iodine, we developed a novel optical parametric amplifier (OPA) [14]. The OPA uses light from an amplified femtosecond Ti:sapphire laser to parametrically amplify the infrared portion of a white light continuum in a beta barium borate (BBO) crystal. The amplified OPA signal pulse is frequency doubled in a second BBO crystal to give a pump pulse that is tunable from 550 to 650 nm, and has a full width at half maximum (FWHM) bandwidth of 15 nm. The pulse is then shaped by propagation through a prism compressor which consists of two glass prisms as shown in Fig. 2. The group velocity dispersion of this arrangement can be made to vary continuously between positive and negative values [15]. By optimally adjusting the distance between the two prisms, a minimum (approximately transform-limited) pulse duration of 49 fs is observed. Then, by translating one of the prisms along its bisector into and out of the optical path, the excitation pulse can be positively or negatively chirped by a precise amount. For more complicated optical wave forms, a pulse tailoring scheme could be used that allows control of both the spectral phase and amplitude profiles [16].

The tailored excitation pulse is sent through a quartz bulb containing iodine vapor at a temperature of 100 °C. To detect the resulting wave packet evolution on the B state, we use the pump-probe laser-induced fluorescence (LIF) technique pioneered for I_2 by Zewail [17], as illustrated in Fig. 1. Other detection methods are possible [18]. An ultrashort probe pulse of a chosen wavelength makes transitions to the higher-lying e state

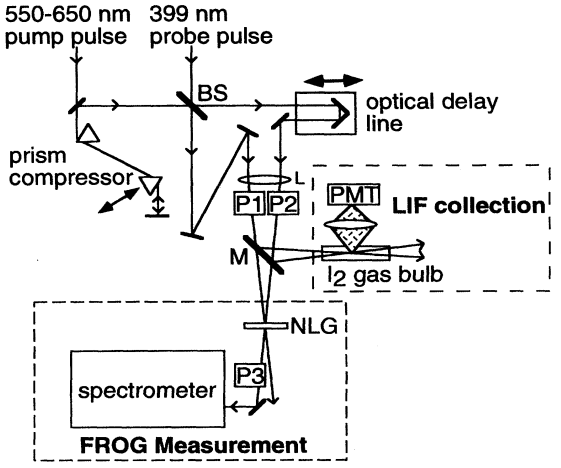

FIG. 2. Experimental apparatus for controlling wave packet dynamics in iodine and measuring the electric field $E(t)$ of the pump and probe pulses by frequency-resolved optical gating (FROG). The LIF signal is recorded with a photomultiplier (PMT) as a function of the optical delay between pump and probe pulses after removing the beam splitter (BS) and using the mirror (M) to direct both pulses into a quartz bulb containing iodine vapor. The lens (L) used to focus the pulses into the cell has a focal length of 25 cm. The chirp of the pump pulse is adjusted by translating one of the prisms of a prism compressor along the direction shown. FROG measurements of $E(t)$ of both pulses are recorded by replacing the beam splitter BS and removing mirror M. Calcite polarizers $P2$ and $P3$ are crossed to form a Kerr gate, while polarizer $P1$ is oriented at 45° with respect to $P2$. The nonlinear gate (NLG) is a 1-mm-thick fused silica plate.

most probable when the wave packet passes through a well-defined region of internuclear distance (that is, the Franck-Condon region, where the laser frequency approximately equals the difference in energy between the e and B states). By detecting the total fluorescence from the e state as a function of the delay time between the excitation and probe pulses, the wave packet density in the probe window at the probe time can be inferred. The precise dependence of the LIF signal on the shape of the wave packet will be analyzed in detail elsewhere [19]. In the present experiment, we frequency double a portion of the Ti:sapphire light to yield a fixed-wavelength probe pulse at 399 nm with an approximate temporal duration of 75 fs. Because the pump and probe pulses are derived from the same Ti:sapphire pulse, synchronization of the pump and probe pulses is excellent.

Accurate pulse characterization is crucial in this experiment, both to adjust the laser system to produce the desired optical wave forms and to compare the results with theory. We use the frequency-resolved optical gating (FROG) technique in which a two-dimensional transform of an ultrashort pulse is measured using an ultrafast optical nonlinear medium [20]. The complete intensity and phase of a pulse, and thus the electric field $E(t)$ as a function of time, can be determined uniquely from the experi-

mentally measured FROG data set using a phase retrieval algorithm [21]. The FROG image provides a fingerprint in time-frequency space that uniquely and intuitively identifies an arbitrarily tailored, coherent light field. As can be seen in Fig. 2, the experiment is designed so that the pump and probe pulses encounter the same material dispersion *en route* both to the fused silica plate used for the FROG measurement and to the iodine sample cell. This experimental geometry ensures that the measured pulse shapes accurately reflect those present in the iodine cell.

To prove that tailoring the pump pulse in an optimal fashion results in control of the vibrational wave packet evolution, we compare the LIF signal resulting from a negatively chirped pulse whose parameters are as close as we could obtain experimentally to the globally optimal field [shown by the dashed contours in Fig. 3(a)] with the LIF signal obtained with a closely related pulse of positive chirp. The positively chirped pulse is expected on theoretical grounds to produce a wave packet that is more delocalized at the target time. To do this, the prism in Fig. 2 is translated out of the beam to negatively chirp the pulse, and the associated LIF signal and FROG image are recorded. Then the prism is translated an equal distance in the opposite direction from the optimal compression (transform-limited, or zero-chirp) point, and the LIF and FROG signals are recorded again.

Figure 3 shows the FROG images for the negatively and positively chirped pulses in a typical experimental run. The FROG inversion routine reveals that these

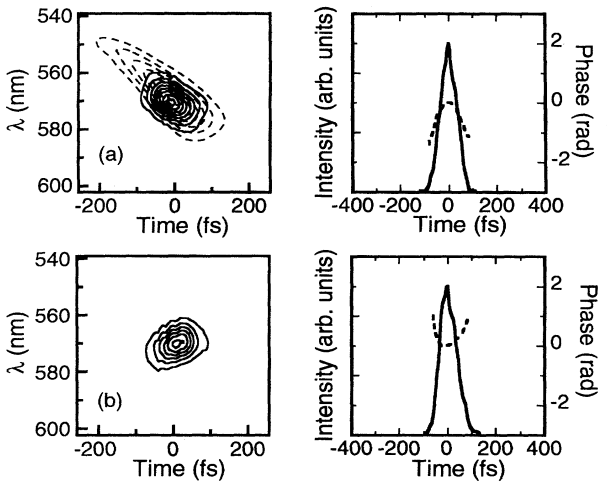

FIG. 3. Experimental FROG signals (solid contours) recorded for the negatively (a) and positively (b) chirped pulses used to generate the LIF signals shown in Fig. 4. The center wavelength of both pulses is 571 nm. The time-dependent intensity (solid curve) and phase (dashed curve) profiles computed from each experimental FROG signal are shown at right. The pulses have approximately equal and opposite linear frequency chirps with an absolute magnitude of 2.3 cm^{-1} fs^{-1}. Also shown in (a) is the computed FROG signal for the theoretical globally optimal reflectron field (dashed contours).

two pulses have identical frequency-domain spectra, and nearly identical intensity versus time profiles. They differ only in how the instantaneous frequency varies with time during the pulse and are, in fact, approximately time reversed with respect to each other. However, as Fig. 4 shows, these two pulses create quite different wave packet dynamics. The first peak in the experimental LIF signals, shown in Fig. 4(a), results when the wave packet passes through the window in internuclear distance opened by the probe pulse as the iodine atoms move apart. The second peak occurs when the atoms move closer together after reflecting from the outer region of the B potential. Our target time, shown by the arrows in Figs. 4(a) and 4(b), was chosen to coincide with the time of this second peak. As seen in Fig. 4(a), the second peak in the LIF signal from the negatively chirped pulse (solid curve) is more narrow and intense than the first peak, corresponding to a more focused wave packet. Conversely, the positively chirped pulse gives rise to an LIF signal (dashed curve) with a second peak which is both weaker and broader, reflecting a more delocalized wave packet during this part of the evolution. We have found that a narrow and intense peak in the LIF signal is a distinct signature of a more focused wave packet in coordinate space [19].

Shown in Fig. 4(b) are the results of quantum mechanical simulations of the LIF signals, using the FROG-derived $E(t)$ for the pump and probe pulses. The calculations include the thermal distribution in the ground (initial) state, and a complete quantum treatment of the influence of pump and probe pulses on the dynamics [19] (that is, we did not invoke the Condon reflection

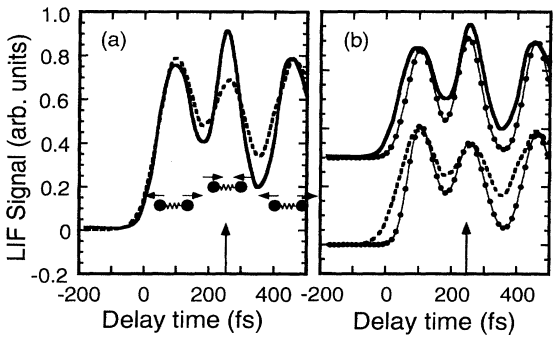

FIG. 4. Experimental demonstration of reflectron quantum control. (a) The second peak of the laser-induced fluorescence (LIF) signals shown here occurs when the iodine atoms are approaching each other after reflecting off the outer part of the potential. The change in height of this peak near the target time at 250 fs indicated by the arrow shows that the wave packet is focused by the negatively chirped pulse (solid curve) and defocused by the positively chirped pulse (dashed curve). (b) Comparison of the experimental data from (a) with theoretical signals (balls connected by thin lines) computed from quantum wave packet propagations which used the measured excitation and probe pulse fields. The curves for the negatively chirped case are displaced vertically for clarity. Again, the arrow marks the target time.

approximation, which assumes that the wave packet evolution during the probe pulse can be neglected). The slower rotational dynamics of the iodine molecule are not included. The agreement with experiment is qualitatively very good.

A comparison of the dashed and solid contours in Fig. 3(a) shows that the pump pulse used in the experiment differs in some respects from the theoretical globally optimal field. In particular, the bandwidth of the experimental pulse is too small by more than a factor of 2. As a consequence, we were unable to make the chirp rate of the experimental pulse large enough to match theory. We observed the greatest yield (defined as the ratio of the heights of the second LIF peak for the negatively and positively chirped pump pulses) by making the chirp rate of the pump pulse as large as experimentally possible. Simulations predict that increasing the bandwidth of the pump pulse by a factor of 2 would lead to a factor of 4 increase in the yield. Modifications to the laser system should allow improved pulse synthesis, and, thus, enable an important investigation of the yield versus pump pulse shape for pulses which are even closer to the theoretically optimal one.

In conclusion, we have controlled the evolution of vibrational wave packets of iodine molecules by properly tailoring an ultrashort laser pulse, in a manner predicted by theory. Control is achieved by using such a tailored pulse to optimally fix the relative phases between the eigenstates of matter. This initial experiment strongly supports theoretical predictions [5–7] that quite general control of nonstationary states is possible with tailored light fields [8]. We would like to stress two points. First, this experiment augments and enhances other pump-probe experiments, such as those by Scherer *et al.* [11] and Zewail and co-workers [12], by incorporating optimal design of the pump field into the experiment. That is, we did not just excite matter with light and observe the results as we changed the properties of the pump pulse. We chose a goal for our material system, predicted the best possible field to reach that goal, and then attempted to best create that field in the laboratory. Second, the control demonstrated here is a special form of control that allows us to localize matter at a time of our choice in a desired region of phase space. Control of this type might be used to control chemical bonding, for example, by using a tailored pump field to focus nuclei about a desired location at a time of our choosing, and then applying a possibly intense additional pulse to selectively and efficiently excite the system to a dissociative surface on which a desired bond is broken [8]. An experiment of this type is being attempted in our laboratory.

[1] W. S. Warren, H. Rabitz, and M. Dahleh, Science **259**, 1581 (1993).
[2] D. J. Tannor and S. A. Rice, J. Chem. Phys. **83**, 5013 (1985).
[3] P. Brumer and M. Shapiro, Ann. Phys. Rev. Chem. **43**, 257 (1992).
[4] M. Demiralp and H. Rabitz, Phys. Rev. A **47**, 809 (1993); R. S. Judson and H. Rabitz, Phys. Rev. Lett. **68**, 1500 (1992).
[5] Y.-J. Yan, R. E. Gillilan, R. M. Whitnell, K. R. Wilson, and S. Mukamel, J. Phys. Chem. **97**, 2320 (1993).
[6] B. Kohler, J. L. Krause, F. Raksi, C. Rose-Petruck, R. M. Whitnell, K. R. Wilson, V. V. Yakovlev, and Y.-J. Yan, J. Phys. Chem. **97**, 12 602 (1993).
[7] J. L. Krause, R. M. Whitnell, K. R. Wilson, Y.-J. Yan, and S. Mukamel, J. Chem. Phys. **99**, 6562 (1993).
[8] B. Kohler, J. L. Krause, F. Raksi, K. R. Wilson, V. V. Yakovlev, R. M. Whitnell, and Y.-J. Yan, Accounts Chem. Res. (to be published).
[9] C. Chen, Y.-Y. Yin, and D. S. Elliott, Phys. Rev. Lett. **64**, 507 (1990).
[10] S. M. Park, S.-P. Lu, and R. J. Gordon, J. Chem. Phys. **94**, 8622 (1991); J. Chem. Phys. **96**, 6613 (1992).
[11] N. R. Scherer, R. J. Carlson, A. Matro, M. Du, A. J. Ruggiero, V. Romero-Rochin, J. A. Cina, G. R. Fleming, and S. A. Rice, J. Chem. Phys. **95**, 1487 (1991).
[12] J. L. Herek, A. Materny, and A. H. Zewail, Chem. Phys. Lett. **228**, 15 (1994).
[13] B. Kohler, J. L. Krause, R. M. Whitnell, K. R. Wilson, V. V. Yakovlev, and Y.-J. Yan, in *Ultrafast Phenomena IX,* edited by G. A. Mourou, A. H. Zewail, P. F. Barbara, and W. H. Knox (Springer-Verlag, New York, 1994), p. 44.
[14] V. V. Yakovlev, B. Kohler, and K. R. Wilson, Opt. Lett. **19**, 2000 (1994).
[15] R. L. Fork, O. E. Martinez, and J. P. Gordon, Opt. Lett. **9**, 150 (1984).
[16] A. M. Weiner, D. E. Leaird, J. S. Patel, and J. R. Wullert, Opt. Lett. **15**, 326 (1990); C. W. Hillegas, J. X. Tull, D. Goswami, D. Strickland, and W. S. Warren, *ibid.* **19**, 737 (1994).
[17] A. H. Zewail, J. Phys. Chem. **97**, 12 427 (1993).
[18] T. J. Dunn, J. N. Sweetser, I. A. Walmsley, and C. Radzewicz, Phys. Rev. Lett. **70**, 3388 (1993).
[19] J. Che, J. L. Krause, M. Messina, K. R. Wilson, and Y. Yan, "Detection and Control of Quantum Molecular Dynamics" (to be published).
[20] R. Trebino and D. J. Kane, J. Opt. Soc. Am. A **10**, 1101 (1993); B. Kohler, V. V. Yakovlev, K. R. Wilson, J. Squier, K. W. DeLong, and R. Trebino, Opt. Lett. (to be published).
[21] K. W. DeLong, D. N. Fittinghoff, R. Trebino, B. Kohler, and K. R. Wilson, Opt. Lett. **19**, 2152 (1994).